

# Sub-10-nm patterning process using directed self-assembly with high $\chi$ block copolymers

Naoko Kihara  
Yuriko Seino  
Hironobu Sato  
Yusuke Kasahara  
Katsutoshi Kobayashi  
Ken Miyagi  
Shinya Minegishi  
Koichi Yatsuda  
Tomoharu Fujiwara  
Noriyuki Hirayanagi  
Hideki Kanai  
Yoshiaki Kawamonzen  
Katsuyoshi Kodera  
Tsukasa Azuma  
Teruaki Hayakawa

# Sub-10-nm patterning process using directed self-assembly with high $\chi$ block copolymers

Naoko Kihara,<sup>a,\*</sup> Yuriko Seino,<sup>a</sup> Hironobu Sato,<sup>a</sup> Yusuke Kasahara,<sup>a</sup> Katsutoshi Kobayashi,<sup>a</sup> Ken Miyagi,<sup>a</sup> Shinya Minegishi,<sup>a</sup> Koichi Yatsuda,<sup>a</sup> Tomoharu Fujiwara,<sup>a</sup> Noriyuki Hirayanagi,<sup>a</sup> Hideki Kanai,<sup>a</sup> Yoshiaki Kawamonzon,<sup>a</sup> Katsuyoshi Kodera,<sup>a</sup> Tsukasa Azuma,<sup>a</sup> and Teruaki Hayakawa<sup>b</sup>

<sup>a</sup>EUVL Infrastructure Development Center, Inc., DSA Research Department, 16-1 Onogawa, Tsukuba-shi, Ibaraki-ken 305-8569, Japan

<sup>b</sup>Tokyo Institute of Technology, Department of Organic and Polymeric Materials, 2-12-1-S8-26 O-okayama, Meguro-ku, Tokyo 152-8552, Japan

**Abstract.** The perpendicularly orientated lamellar structure of the self-organized diblock copolymer is an attractive template for sub-10-nm line-and-space pattern formation. We propose a method of evaluating the neutral layer (NL) whose performance has an important bearing on the perpendicular orientation of the lamellar structure. The random copolymer of methyl methacrylate and *t*-butyl POSS methacrylate (MAIBPOSS) has been investigated as an NL for a polymethylmethacrylate-*b*-polymethacrylethylPOSS (PMMA-*b*-PMAIBPOSS) lamellar structure. PMMA-*b*-PMAIBPOSS material has the potential to form sub-10 nm line-and-space pattern, in addition to high etch selectivity due to its POSS structure. Under the free surface, PMMA-*b*-PMAIBPOSS film on the random copolymer layer showed horizontal orientation. However, a half-pitch of a 7-nm finger pattern structure was observed by peeling off the horizontally oriented layer. The upper portion of the PMMA-*b*-PMAIBPOSS film was eliminated till proximity of the random copolymer layer by CF<sub>4</sub> gas etching. From the result, it was revealed that the PMMA-*r*-PMAIBPOSS works as an NL. It was confirmed that the contact angle analysis using an appropriate polymer is a suitable method for evaluation of the surface energy performance of the copolymer with the attribute of high segregation energy. © The Authors. Published by SPIE under a Creative Commons Attribution 3.0 Unported License. Distribution or reproduction of this work in whole or in part requires full attribution of the original publication, including its DOI. [DOI: [10.1117/1.JMM.14.2.023502](https://doi.org/10.1117/1.JMM.14.2.023502)]

Keywords: directed self-assembly; lithography; self-organization; lamella; neutral layer.

Paper 14148 received Oct. 9, 2014; accepted for publication Mar. 12, 2015; published online Apr. 9, 2015.

## 1 Introduction

Directed self-assembly (DSA) lithography, which combines self-assembling materials and lithographically defined prepatterns, is a candidate to extend optical/EUV lithography beyond sub-10 nm.<sup>1,2</sup> DSA of block copolymer (BCP) films on chemically or topologically patterned substrates is an attractive patterning technique that combines the ability of BCPs to self-assemble into nanoscale features with the use of lithographic tools.<sup>3–7</sup> One of the important problems concerning practical application of DSA lithography is a “defect” problem. So far, the typical defect densities remain orders of magnitude away from the target concentration of 0.01 defects/cm<sup>2</sup> proposed by the International Technology Roadmap for Semiconductors.<sup>8</sup> Therefore, it is crucially important to minimize defect levels and maximize DSA lithography process margin by carefully designing lithographically defined prepatterns and precisely adjusting process conditions. Applying polystyrene-polymethylmethacrylate (PS-*b*-PMMA) diblock copolymer in a full-pitch size of around 25 nm, such a defect investigation has been reported.<sup>9</sup> On the other hand, the domain size of self-organization is basically determined by the Flory–Huggins  $\chi$  parameter and the polymerization index.<sup>10,11</sup> To realize sub-10 nm feature size patterns, a higher  $\chi$  parameter diblock copolymer is required. For example, polystyrene-*b*-poly 2-vinylpyridine and polystyrene-*b*-polydimethylsiloxane are well known as high  $\chi$  materials with a potential for

sub-10 nm patterns.<sup>12–14</sup> However, to apply such materials for the lithographic process, high etching selectivity between the two composite polymers is required in order to transfer the pattern to the substrate.<sup>15</sup> In this work, we report a fabrication process of sub-10 nm line-and-space patterns using the DSA materials featuring high  $\chi$  parameter and high etch selectivity. We applied one of the most promising DSA materials, namely, POSS containing DSA materials, to realize sub-10 nm line-and-space patterning processes.<sup>16</sup> In addition, we report the evaluation process of a new neutral layer (NL) material for Si containing high  $\chi$  material.

## 2 Experimental Methods

### 2.1 Materials

The BCP materials utilized in this work are listed in Table 1. The cylindrical and lamellar phase-separation materials utilized were polymethylmethacrylate-*b*-polymethacrylethylPOSS (PMMA-*b*-PMAEtPOSS) and polymethylmethacrylate-*b*-polymethacryli-butylPOSS (PMMA-*b*-PMAIBPOSS). PMMA-*b*-PMAEtPOSS and PMMA-*b*-PMAIBPOSS were synthesized by living anionic polymerization.<sup>17,18</sup> The domain sizes of microphase separation listed in Table 1 were obtained by bulk small angle x-ray scattering measurements. As the NL material, polymethylmethacrylate-*r*-polymethacryli-butylPOSS-*r*-polyglycidylmethacrylate (PMMA-*r*-PMAIBPOSS-*r*-PGMA) was utilized. The NL materials were synthesized by a reversible addition-fragmentation chain transfer (RAFT) polymerization method using 2-phenyl-2-propyl benzodithioate as an initiator.<sup>19</sup> The PMAIBPOSS volume in the

\*Address all correspondence to: Naoko Kihara, E-mail: [naoko.kihara@eidc.co.jp](mailto:naoko.kihara@eidc.co.jp)

**Table 1** Block copolymer materials and neutral layer (NL) materials.

Structure	Polymer	Mn	Mw/Mn	PMAPOSS	d (nm)
Cylinder	PMMA <sub>54</sub> - <i>b</i> -PMAEtPOSS <sub>10</sub>	13,200	1.06	59 (wt.%)	11.2
Lamella	PMMA <sub>123</sub> - <i>b</i> -PMAIBPOSS <sub>7</sub>	19,000	1.04	35 (wt.%)	14.8
NL	PMMA- <i>r</i> -PMAPOSS- <i>r</i> -PGMA	36,700	1.25	43 (vol.%)	—
NL	PMMA- <i>r</i> -PMAIBPOSS- <i>r</i> -PGMA	25,000	1.35	52 (vol.%)	—
NL	PMMA- <i>r</i> -PMAIBPOSS- <i>r</i> -PGMA	24,000	1.18	57 (vol.%)	—
NL	PMMA- <i>r</i> -PMAIBPOSS- <i>r</i> -PGMA	67,000	1.37	61 (vol.%)	—

random polymer was varied from 52% to 61%. Mn and polydispersity index (PDI = Mw/Mn) were measured by gel permeation chromatography. BCP composition was determined by nuclear magnetic resonance (NMR) spectrum measurement. The volume of NL polymer composition was calculated from the composition ratio determined by NMR spectrum.

## 2.2 Preparation Process of DSA

Graphoepitaxy guide of patterned spin-on-glass (SOG) substrate was prepared as follows. A substrate consisting of a 100-nm thick layer of SOG was formed on a Si wafer. SOG material was supplied from a resist vendor. A Clean TRACK™ ACT12™ (Tokyo Electron Ltd.) was used for SOG coating, baking, and rinsing. On the SOG film, and a commercially available ArF immersion photoresist was coated. A Clean TRACK™ LITHIUS™ (Tokyo Electron Ltd.) was used for the ArF immersion photoresist coating, baking, and development. An NSR-S610C (Nikon Corp., 1.3NA) ArF excimer laser immersion scanner was used for exposures. Using the photoresist pattern as an etching mask, SOG film was etched to form 10-nm depth trenches by CF<sub>4</sub> gas. A TACTRAS™ SCCM-T4™ (Tokyo Electron Ltd.) chamber was used for guide pattern etching. The photoresist pattern was removed by O<sub>2</sub> plasma ashing.

PMMA-*b*-PMAPOSS film was prepared as follows. A propylene glycol monomethyl ether acetate (PGMEA) solution of 1 wt.% of BCP was prepared. The BCP film was formed by spin-coating on a bare Si wafer or patterned SOG substrate and then annealed in an oven at 150°C for 12 h under a vacuum of 5 Torr. For these experiments, 2 cm<sup>2</sup> chips of bare Si or patterned SOG substrate were used. A SPINCOATER 1H-HD (MIKASA Co., Ltd) was used for BCP and NL coating. The NL was prepared using PMMA-*r*-PMAIBPOSS-*r*-PGMA. PGMA units were added to the NL for crosslinking that improves the chemical compatibility of the NL for the subsequent BCP casting step. A PGMEA solution of 1 wt.% of the random copolymer was prepared. The prepared solution was spin-coated onto an Si wafer. The obtained thickness was 13 nm. After baking at 150°C for 12 h under a vacuum of 5 Torr, the film was rinsed with PGMEA to remove uncrosslinked polymer chains. The remained film thickness was ~3 to 5 nm. The etching of BCP film was carried out using CF<sub>4</sub> gas and O<sub>2</sub> gas. An inductive coupled plasma (ICP) etcher, Multiplex ICP (Surface

Technology Systems) was utilized as an etching instrument. The platen/coil power was tuned to be 50 W/50 W. For CF<sub>4</sub> gas etching and O<sub>2</sub> gas etching, chamber process pressure was controlled to be 5 and 0.6 mTorr, respectively.

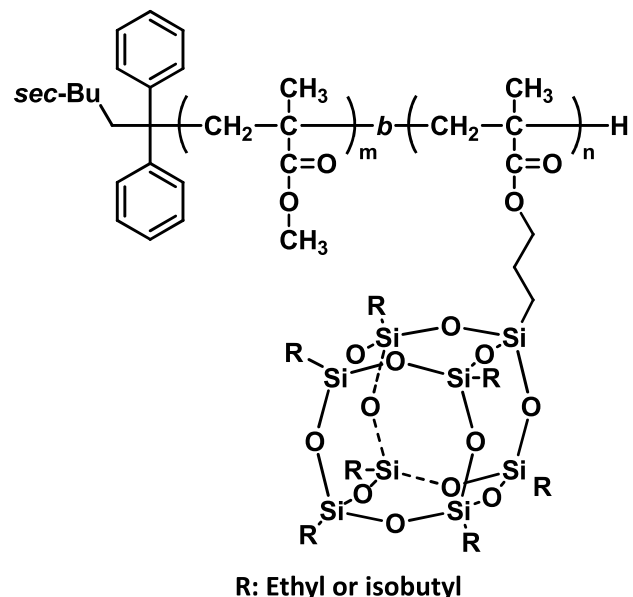
## 2.3 Measurements

Scanning electron microscope (SEM) images were observed using SU9000 (Hitachi High-Technologies Corp.). To observe the film surface image, an atomic force microscope (AFM, Veeco Metrology Group) was utilized. The water contact angle was measured by a self-made instrument. The contact angle of PMMA was measured as follows.<sup>20</sup> Thin PMMA film of 18-nm thickness was coated on an NL. Then the film was heated at 170°C for 15 h under a vacuum of 5 Torr. The contact angle of the PMMA dot was measured by AFM.

## 3 Results and Discussion

### 3.1 Performance of Si-Containing BCP Materials

PS-PMMA has been investigated for application of fine line-and-space pattern formation. PS-PMMA has several advantages as the DSA material; the etching selectivity of PS and

**Fig. 1** Chemical structure of block copolymer (BCP).

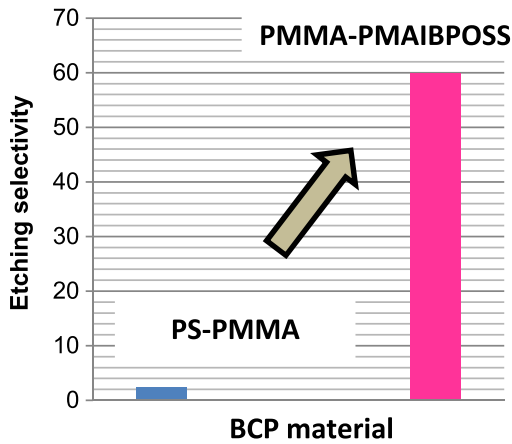


Fig. 2 O<sub>2</sub> gas etch selectivity of BCPs.

PMMA is high for an organic BCP material, and the relatively low segregation energy enables perpendicular orientation of lamellar structure in a normal ambience without any special atmosphere or top coat.<sup>9,15</sup> However, to obtain a sub-10 nm feature pattern by DSA, new materials with a high  $\chi$  parameter are required.

Figure 1 shows the chemical structure of the BCPs utilized in this work. In Table 1, the composition of BCPs

and their d-spacing is listed. As shown in the d-spacing figures, this BCP structure has the potential to form a sub-10 nm line pattern template. In the device fabrication process, the fine pattern of DSA should be transferred to the Si substrate. For the transfer process of such a fine pattern to a substrate, the performance of dry etching selectivity is important. Figure 2 shows O<sub>2</sub> gas etching selectivity of PMMA and PMAIBPOSS compared with that of PS and PMMA. The durability of PMAIBPOSS to O<sub>2</sub> etching is high and the etch selectivity to PMMA is about 60, whereas PS-PMMA stays around 2 to 3.<sup>15</sup>

Figure 3 shows the graphoepitaxy process of cylindrical PMMA-*b*-PMAEtPOSS material. The guide pattern was prepared by SOG material on an Si substrate using an ArF lithography process. The height of SOG guide wall was designed to be 10 nm. To avoid multiple-layer formation of BCP in the trench, the depth of the trench was designed to be same as the d-spacing of cylinder BCP. The thickness of the BCP film was determined by pretest coating on Si substrate. The thickness of the BCP film on an Si substrate was 9.2 nm. The SEM images of annealed BCP in the guide pattern were shown in Fig. 4. As shown in Fig. 4(b), a half-pitch of 7 nm was obtained. However, several types of defects were observed in one test chip. Figure 5 shows the SEM images of the typical defect type observed in one test chip. Both a nonfill defect and overflow defect exist on one test chip. The observed chip was prepared by applying the

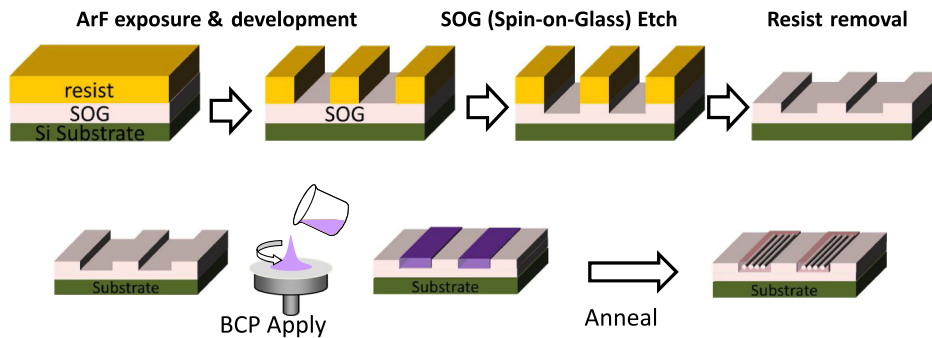


Fig. 3 Guide preparation and applying BCP process image.

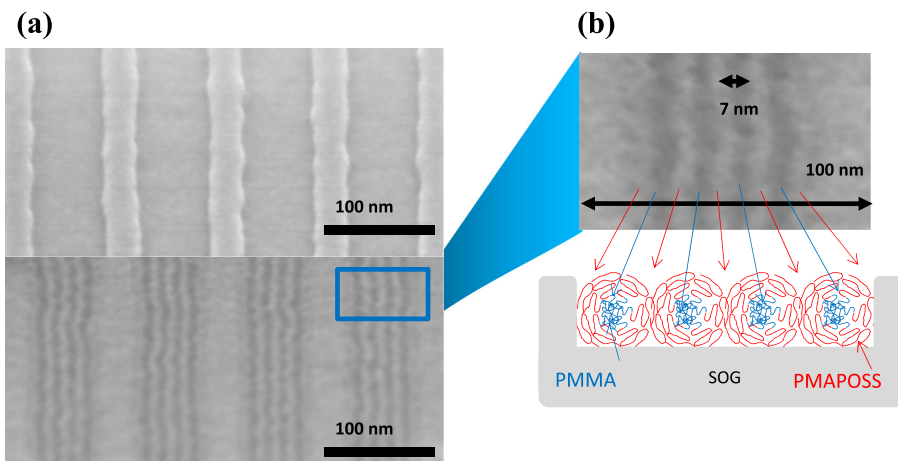
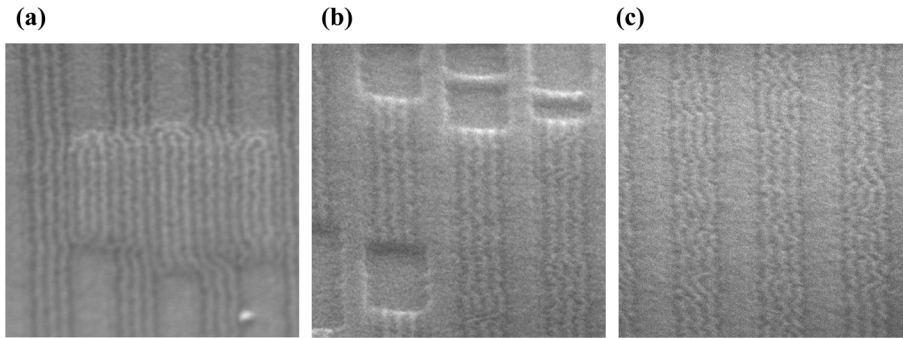
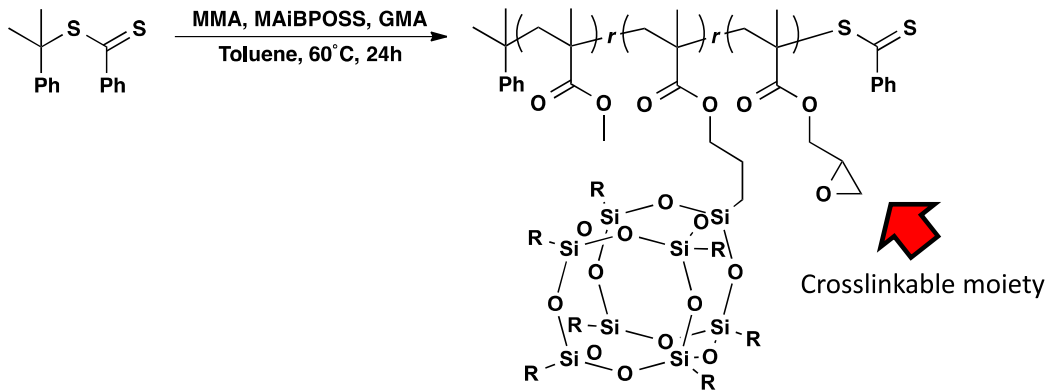


Fig. 4 Scanning electron microscope (SEM) images of graphoepitaxy guide pattern and PMMA54-*b*-PMAEtPOSS10 in trench guide. (a) Top-down SEM images of guide pattern and BCP in trench and (b) magnified SEM image and schematic image of cross section.



**Fig. 5** SEM images of defects observed in one test chip. (a) BCP overflow, (b) nonfilled, and (c) line-edge roughness.



**Fig. 6** Scheme of PMMA-*r*-PMAIBPOSS-*r*-PGMA preparation.

same process shown in Fig. 3. This indicates that, in applying a cylindrical structure for line-and-space pattern formation, coating-process control is essential to remove such defects. One of the advantages of applying the perpendicular lamellar structure is that less care is needed to be exercised for measures to deal with such defects.

### 3.2 Neutral Layer Material Preparation for Perpendicular Orientation of Lamellar Structure

To obtain a perpendicular orientation of the lamellar BCP pattern, the surface energy of the substrate should be controlled to have an equal affinity for both polymers. In the case of PS-*b*-PMMA, random copolymers of PS and

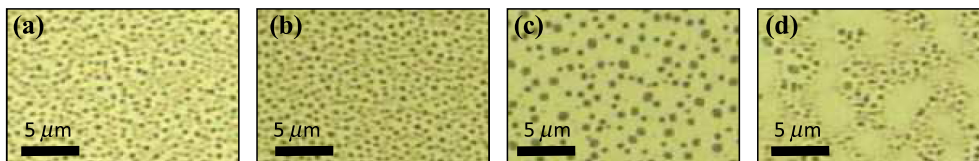
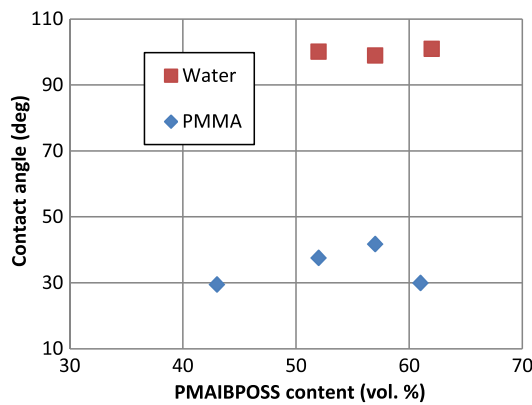


**Fig. 7** Water and PMMA contact angles on PMMA-*r*-PMAIBPOSS-*r*-PGMA film surface and photographs of PMMA dots on the random copolymers. (a) PMAIBPOSS content 43%, (b) 52%, (c) 57%, and (d) 61%.

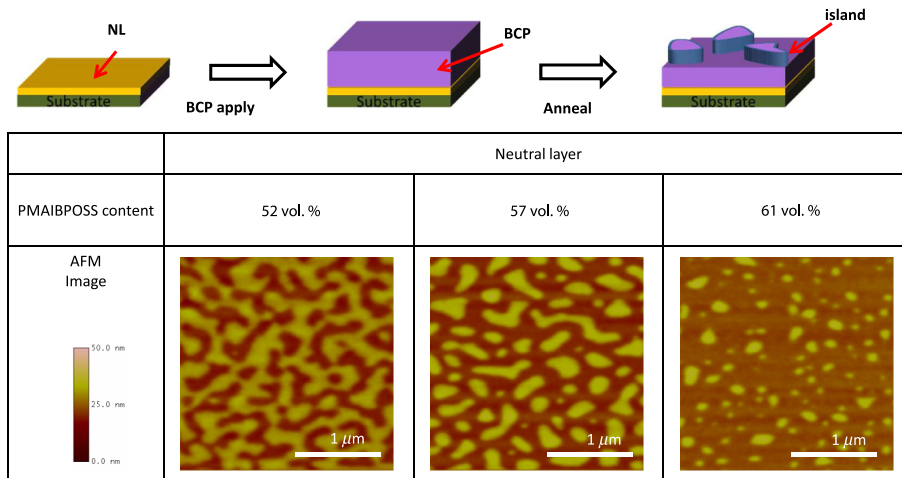


**Fig. 8** Atomic force microscope (AFM) images of annealed BCP film surfaces and schematic image of BCP on PMMA-*r*-PMAIBOSS-*r*-PGMA films.

PMMA were applied.<sup>20,21</sup> When the composition ratio of PS and PMMA of the random copolymer matched the BCP composition, perpendicular orientation was obtained. To form a perpendicularly oriented PMMA-*b*-PMAIBOSS's lamellar structure, random copolymers of PMMA and PMAIBOSS were prepared as NL materials. The chemical structure of the NL material is shown in Fig. 6. The RAFT polymerization method was used for the polymerization. A cross-linkable component, glycidylmethacrylate, was added to the copolymer composition to avoid the intermixing when the BCP was coated on the random copolymer layer.

Three neutral materials, whose PMAIBOSS volume content was varied from 52% to 61%, were synthesized. The neutral substance surface was prepared as follows. Random copolymer film was formed on a substrate by spin coating. The film was baked to crosslink glycidyl groups. To eliminate uncrosslinked polymer, the film was rinsed with

PGMEA. The surface energy performance of the random copolymers was examined by the measurement of water and PMMA contact angles.<sup>17</sup> The obtained contact angles of the random copolymer films are shown in Fig. 7. A significant difference is not observed in water contact angles, which is considered attributable to high water repellency resulting from POSS. On the other hand, contact angles of the PMMA dot show significant change according to the PMAIBOSS content. The contact angle of the PMMA dot increases with an increase of the PMAIBOSS content, except in the case of 61% content. The photographs of PMMA dots on NLs are shown in Fig. 7. As shown in the photographs, the shape of the PMMA dot structure on 61% PMAIBOSS content film is different to that on the films with less PMAIBOSS content. The low contact angle of the PMMA dot on the high PMAIBOSS content film was caused by the degradation of the PMMA dot shape.

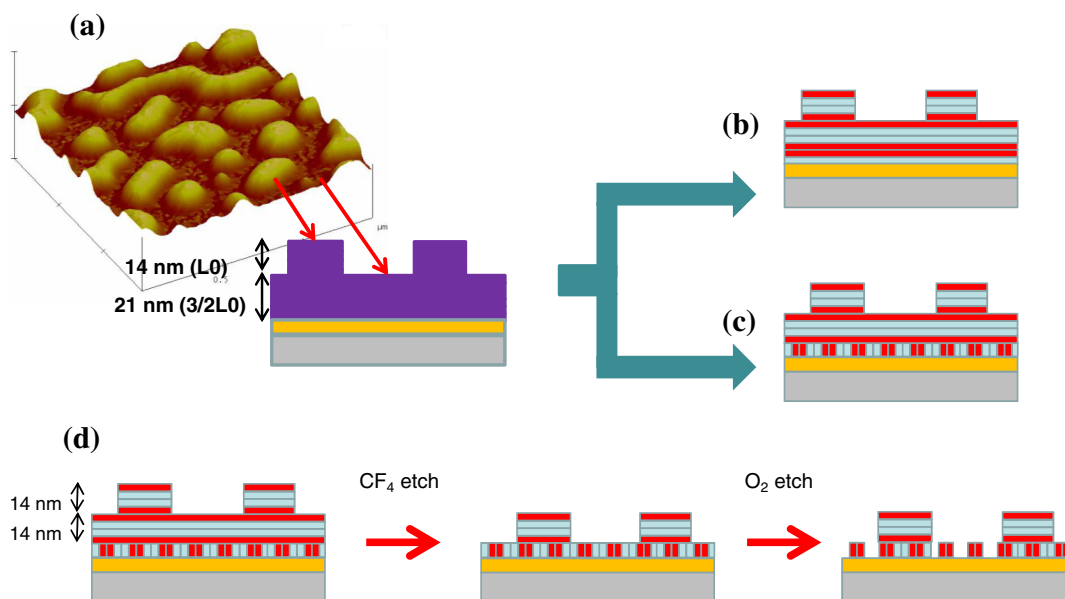


**Fig. 9** Expected images of phase-separation structure of BCP on NL and schematic image of dry development process. (a) AFM image and schematic image, (b) horizontal orientation, (c) partially perpendicular orientation, and (d) examined etch process.

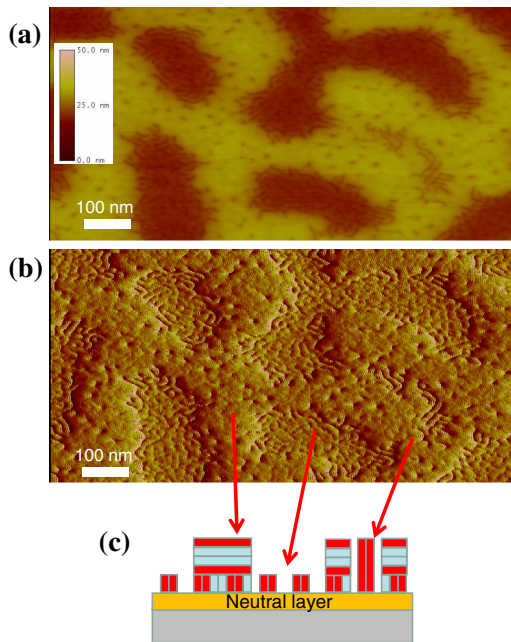


**Fig. 10** Atomic force microscope images of etched BCP film surface. (a) Height image, (b) amplitude image, and (c) schematic image of cross section.

### 3.3 Observation of PMMA-*b*-PMAIBPOSS Lamellar Structure on the Neutral Layers

On the prepared random copolymer layer, BCP film was formed and annealed. Figure 8 shows the AFM images of annealed BCP film surfaces. As shown in these figures, an island structure is observed. The height of the island is 14 nm, which is consistent with  $L_0$ . The island area decreased with increasing the PMAIBPOSS content of PMMA-*r*-PMAIBPOSS-*r*-PGMA although the BCP coating condition was the same. That means that the film thickness of BCP was affected by the surface condition caused by the PMAIBPOSS content. Usually, such an island structure is considered indirect evidence of the horizontal orientation of the lamellar structure under a free surface (Fig. 9). To observe the orientation of the lamellar structure just above the random copolymer layer, the horizontally oriented

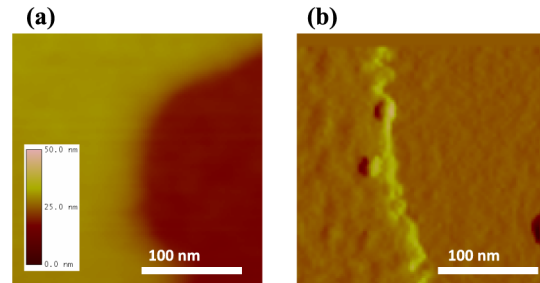


**Fig. 12** BCP behavior on bare Si wafer. (a) Height image of annealed BCP film and (b) amplitude image of etched film.

upper layer was eliminated by dry etching with  $CF_4$  gas and  $O_2$  gas.

Figure 10 shows the AFM images of the etched BCP film surface. As shown in this figure, the finger pattern is observed aside from the horizontally oriented lamellar structure in proximity to the random copolymer surface. The cross-sectional schematic image of the etched film is also illustrated in Fig. 10. In the brightly colored area (horizontally oriented lamellar area) of the AFM height image, a finger pattern, which is considered to indicate partial penetration of the perpendicular lamellar structure, is observed [Fig. 10(a)]. This experimental result indicates that the lamellar structure of the BCP on the random copolymer surface oriented perpendicularly. However, the effect did not reach the BCP film surface.

Figure 11 shows the BCP behavior dependence on the random copolymer layer whose PMAIBPOSS composition volume ratio was varied from 52% to 61%. As shown in this figure, BCP on the 52% and 57% PMAIBPOSS content copolymers shows a finger pattern. The behavior of the BCP on a bare Si wafer was shown in Fig. 12. The film thickness of the coated BCP on the Si was 19 nm. Annealing and etching were applied the same processing as the BCP film on the NL. As shown in Fig. 12, no finger pattern was observed on the etched film.

These results proved that PMMA-*r*-PMAIBPOSS-*r*-PGMA performs as a neutral material for PMMA-*b*-PMAIBPOSS. The perpendicular control of the bottom layer was accomplished by the NL. However, the top surface orientation of the BCP film was still under the influence of

	Neutral layer		
PMAIBPOSS content	52 vol. %	57 vol. %	61 vol. %
AFM image			

**Fig. 11** BCP behavior dependence on neutral layer composition.

the free surface. For application of the lithographic process, control of the top surface energy is required in order to obtain the perfect perpendicular orientation.<sup>22</sup>

#### 4 Summary

Perpendicular orientation of lamellar PMMA-*b*-PMAIBPOSS material was investigated. The performance of PMMA-*r*-PMAIBPOSS-*r*-PGMA as an NL for PMMA-*b*-PMAIBPOSS was clarified by observation of the proximity area on the PMMA-*r*-PMAIBPOSS-*r*-PGMA layer. In this study, it was verified that the contact angle analysis using a proper polymer is an appropriate method for evaluation of the surface energy performance of copolymer with the attribute of high segregation energy. For an application of the lithographic process, control of the top surface energy is required in order to obtain the perfect perpendicular orientation.

#### Acknowledgments

A part of this work was funded by the New Energy and Industrial Technology Development Organization (NEDO) under the EIDEC project.

#### References

1. J. Bang et al., "Block copolymer nanolithography: translation of molecular level control to nanoscale patterns," *Adv. Mater.* **21**, 4769 (2009).
2. J. Y. Cheng et al., "Templated self-assembly of block copolymers: top-down helps bottom-up," *Adv. Mater.* **18**, 2505 (2006).
3. J. Y. Cheng et al., "Dense self-assembly on sparse chemical patterns: rectifying and multiplying lithographic patterns using block copolymers," *Adv. Mater.* **20**, 3155 (2008).
4. M. P. Stoykovich et al., "Directed assembly of block copolymer blends into nonregular device-oriented structures," *Science* **308**, 1442 (2005).
5. R. Ruiz, R. L. Sandstrom, and C. T. Black, "Induced orientational order in symmetric diblock copolymer thin films," *Adv. Mater.* **19**, 587 (2007).
6. K. Naito et al., "2.5-inch disk patterned media prepared by an artificially assisted self-assembling method," *IEEE Trans. Mag.* **38**, 1949 (2002).
7. T. Yamaguchi and H. Yamaguchi, "Two-dimensional patterning of flexible designs with high half-pitch resolution by using block copolymer lithography," *Adv. Mater.* **20**, 1684 (2008).
8. "International technology roadmap for semiconductors," <http://www.itrs.net/home.html> (2008).
9. C. Bencher et al., "Self-assembly patterning for sub-15 nm half-pitch: a transition from lab to fab," *Proc. SPIE* **7970**, 79700F (2011).
10. T. Ohta and K. Kawasaki, "Equilibrium morphology of block copolymer melts," *Macromolecules* **19**, 2621 (1986).
11. F. S. Bates and G. H. Fredrickson, "Block copolymer thermodynamics: theory and experiment," *Annu. Rev. Phys. Chem.* **41**, 525 (1990).
12. C. A. Ross et al., "Si-containing block copolymers for self-assembled nanolithography," *J. Vac. Sci. Technol. B* **26**, 2489 (2008).
13. N. Kihara et al., "Fabrication of 5 Tdot/in.2 bit patterned media with servo pattern using directed self-assembly," *J. Vac. Sci. Technol. B* **30**, 06FH02 (2012).
14. H. Yoshida et al., "Topcoat approaches for directed self-assembly of strongly segregating block copolymer thin films," *J. Photopolym. Sci. Technol.* **26**, 55 (2013).
15. K. Asakawa and T. Hiraoka, "Nanopatterning with microdomains of block copolymers using reactive-ion etching selectivity," *Jpn. J. Appl. Phys.* **41**, 6112 (2002).
16. H. Yoshida et al., "Directed self-assembly with density multiplication of cage silsesquioxane-containing block copolymer via controlled solvent annealing," *J. Photopolym. Sci. Technol.* **24**, 557 (2011).
17. T. Hirai et al., "Hierarchical nanostructures of organosilicate nanosheets within self-organized block copolymer films," *Macromolecules* **41**, 4558 (2008).
18. C. Chiou et al., "Hydrogen bond interactions mediate hierarchical self-assembly of POSS-containing block copolymers blended with phenolic resin," *Macromolecules* **47**, 8709 (2014).
19. J. Chiefari et al., "Living free-radical polymerization by reversible addition-fragmentation chain transfer: the RAFT process," *Macromolecules* **31**, 5559 (1998).
20. P. Mansky et al., "Controlling polymer-surface interactions with random copolymer brushes," *Science* **275**, 1458 (1997).
21. S. Ham et al., "Microdomain orientation of PS-*b*-PMMA by controlled interfacial interactions," *Macromolecules* **41**, 6431 (2008).
22. C. M. Bates et al., "Polarity-switching top coats enable orientation of sub-10-nm block copolymer domains," *Science* **338**, 775 (2012).

**Naoko Kihara** received her MS degree in photochemistry from Ochanomizu University. She joined Toshiba Corporation in 1983 and has been working on organic materials for fabrication electric devices. Since 2013, she has been working for DSA development program in EUVL Infrastructure Development Center, Inc. Currently, she is in DSA Research Department for DSA process development.

Biographies of the other authors are not available.